Harnessing Telodendrimer Nanotraps in Nanogels for Systemic Immune Modulation in Sepsis Treatment

Xiaotian Ji[1], Changying Shi[1], DeKai Yuan[1], Liye Suo[2], Xiguang Yang[1], Dandan Guo[1,4], Norifumi Urao[1,4], Robert N. Cooney[3,4], Juntao Luo[1,3,4,5,6]*

[1] Department of Pharmacology, [2] Department of Pathology, [3]Department of Surgery, [4]Upstate Sepsis Interdisciplinary Research Center, [5]Department of Microbiology and Immunology, [6]Upstate Cancer Center, State University of New York Upstate Medical University, Syracuse, NY 13210, United States

*Luoj@upstate.edu

Abstract

Sepsis is featured by the uncontrolled life-threatening systemic inflammatory responses to infection and tissue damages. Spontaneous attenuation of a broad spectrum of septic molecules and cytokines is promising for effective sepsis treatment. We have developed functionalized nano-sized hydrogel, i.e., nanogel (NG), via a one-pot precipitation polymerization using biocompatible, biodegradable monomers/crosslinkers and versatile polymerizable functional telodendrimer (TD) nanotraps (NTs) for effective scavenging of septic molecules. The telodendrimer nanogel (TD-NG) has spherical morphology with homogenous size distribution around 300 nm. TD-NG is stable in plasma and can be degraded in the presence of reducing agents, e.g. intracellular glutathione. The size-exclusive nanogel network and the polyethylene glycol (PEG) shell coating exclude the abundant serum proteins for selective and effective capture of septic molecules, e.g., LPS, TNF-α, IL-1β, IL-6. PEGylated TD-NGs are nontoxic in cell culture with low immune cell uptake, and biocompatible after i.v. injection with prolonged circulation time and majority elimination into feces via liver-bile ducts. Systemic administration of TD-NG significantly inhibits the LPS-induced NF-κB activation and cytokine production. PEGylated TD-NGs effectively attenuate inflammatory molecules *in situ* for effective immune modulation, which ameliorate tissue damage and improve the survival rate in severe sepsis mouse models induced by cecum ligation and puncture.

Keywords: Nanogel, telodendrimer nanotrap, cytokine adsorption, endotoxin removal, immune modulation, sepsis treatment.

Introduction

Sepsis is a life-threatening clinical complication of infection and/or tissue damages characterized by uncontrolled systemic inflammatory response.[1] Despite huge efforts devoted to finding an effective therapy, the mortality rate in sepsis remains high, and the number of hospitalizations resulting from this condition continues to rise.[2] Lipopolysaccharide (LPS) or endotoxin is a major constituent of the outer cell wall of Gram-negative bacteria and is strongest immune stimulating compounds in nature.[3] Upon entering the blood circulation, it may induce systemic inflammation and sepsis.[4] Emerging evidence suggests that the systemic spread of endotoxin from sites of infection, rather than bacteremia itself, is crucial in the pathogenesis of this dramatic immune dysregulation.[5,6] LPS activates various immune cells to produce potent pro-inflammatory cytokines, e.g., tumor necrosis factor (TNF), interleukin-1 (IL-1), IL-6, and IL-8, and nitric oxide (NO).[7] During the infection and tissue damages, the release of pathogen associated molecular patterns (PAMPs) and damage associated molecular patterns (DAMPs) perpetuates systemic inflammatory response, which result in overproduction of cytokines in serum and tissues and lead to multiple-organ failures.[8,9] Therefore, timely intervention to reducing systemic circulating endotoxin and inflammatory cytokines is beneficial for managing sepsis.

LPS consists of a hydrophobic membrane-anchoring lipid A moiety, which have a bisphosphoryl diglucosamine backbone with multiple pendant fatty acid chains.[10] Interestingly, most proinflammatory cytokines are negatively charged proteins[11] with medium size in molecular weights (mostly less than 30 kDa).[12] Thus, the combination of ionic and hydrophobic interactions may be effective strategy in designing of bio-scavengers to sequester both endotoxins and proinflammatory cytokines to control inflammation. We have developed a series of novel PEGylated linear-dendritic telodendrimer nanocarriers comprising multiple charges and hydrophobic moieties on the flexible periphery for effective protein delivery.[13-15] Further, we

conjugated telodendrimer nanotrap (TD NT) in a size-exclusive hydrogel resin, which exhibits high efficacy in absorbing LPS and cytokines with both charge and size selectivity. TD NT hydrogel resin has demonstrated a 100% survival benefit when combined with low dose antibiotics in a severe sepsis mouse model,[16] which can be packed in hemoperfusion cartridge for clinical sepsis treatment. Based on these studies, we further developed an injectable core-shell hydrogel nanoparticle (200-300 nm) with TD NT conjugated in the core for selective adsorption of septic molecules *in vitro* and *in vivo*.[17] Similar nanogel nanotrap based on rigid charged aromatic molecular bites has been developed for *in vitro* application to concentrate small and medium sized molecules in biofluid for biomarker analysis.[18-20] However, the poor biocompatibility and biodegradability of these nanogel nanotrap made by conventional thermal sensitive polymers, e.g., PNIPAM, raise significant concerns for intravenous administration. The scavenge of immune-stimulating and immune-signaling molecules in blood circulation by hemoperfusion approaches remains promising; however, the attenuation of these pathogenic molecules from blood circulation and spontaneously in vital organ and tissue is critical to control the hyperinflammation effectively and prevent tissue damages in sepsis, which is unmet in the clinic sepsis treatment.

Herein, we directly integrate polymerizable TD NT into biodegradable and biocompatible PEGylated nanogel via a one-pot precipitation polymerization. The polyethylene glycol (PEG) on TD NT displays on the surface to stabilize nanogel and reduce the non-specific binding. The crosslinking degree of nanogel can be fine-tuned to optimize the size exclusive effects for selective cytokine/endotoxin capture in the core of the nanogel by TD NT (**Scheme 1**). The nanogels have low cytotoxicity and high biocompatibility and long circulation time *in vivo* for effective sequestration of bacterial endotoxin and proinflammatory cytokines in treating severe sepsis mouse models. TD NT nanogel promises a novel injectable immune modulating therapy for sepsis treatment.

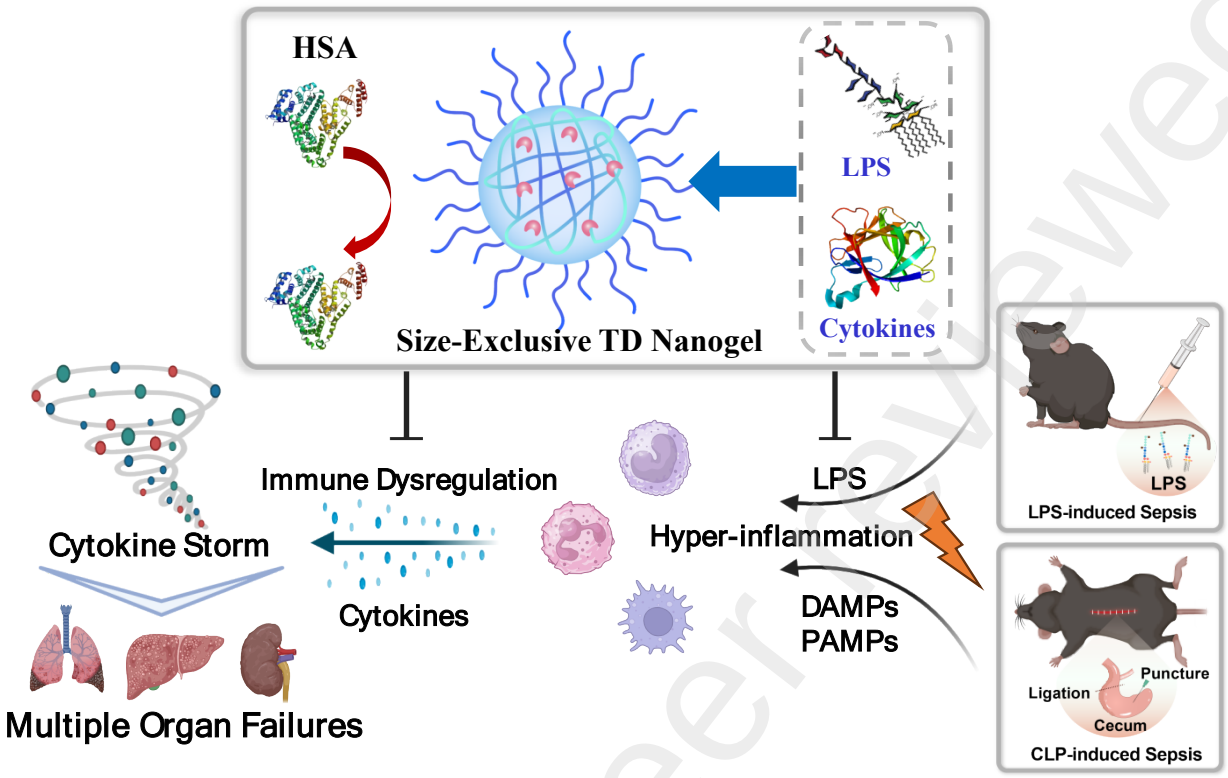

Scheme 1. Schematic illustration of the design and mechanism for TD-NG to prevent the cytokine storm and multiple organ failure via scavenging endotoxin and pro-inflammatory cytokines simultaneously in sepsis mouse models induced by LPS injection or cecum ligation and puncture procedure.

Methods

Materials. The following chemicals were used in the study: Monomethyl-terminated poly(ethylene glycol) monoamine hydrochloride (MeO-PEG-NH_2·HCl, Mw 5 kDa) purchased from JenKem Technology USA Inc. Heptadecanoic acid (C17, 98%) purchased from TCI. N, N'-methylenebis(acrylamide) (BIS, 99%), lithium hydroxide (anhydrous, 98%), and succinic anhydride (99%) obtained from Alfa Aesar. (Fmoc)-Lys(Fmoc)-OH, (Fmoc)-Lys(Dde)-OH, (Fmoc)-Lys(Boc)-OH, and trifluoroacetic acid (TFA) purchased from Chem-Impex International, Inc. (Fmoc)-Arg(Pbf)-OH purchased from AnaSpec Inc. N, N'-diisopropylcarbodiimide (DIC), N-hydroxybenzotriazole (HOBt), N-dimethylformamide, anhydrous (DMF, 99.8%), methylene chloride (DCM), methanol (MeOH), potassium persulfate

(KPS), and glutathione (GSH, 98%) received from Acros Organics. Cystamine dihydrochloride (98%) purchased from Fluka. Triethylene glycol methyl ether methacrylate (TEGMMA, contains MEHQ as inhibitor, 93%), triethylamine (TEA), N,N-Diisopropylethylamine (99%), Tris(2-carboxyethyl)phosphine hydrochloride (TCEP), 2-Iodoacetamide, Rhodamine B (95%), hydrazine hydrate, acryloyl chloride, α-lactalbumin (α-LA from bovine milk), and LPS from Escherichia coli (L4130) purchased from Sigma-Aldrich. Tetrazolium compound [3-(4,5-dimethylthiazol-2-yl)-5-(3-carboxymethoxyphenyl)-2-(4-sulfophenyl)-2H-tetrazolium, MTS] and phenazine methosulfate purchased from Promega. ELISA kits purchased from Invitrogen for direct use.

Synthesis of telodendrimers (TDs). The charged and hydrophobic TDs were synthesized using MeO-PEG^{5k}-NH_2·HCl (5 kDa) via a solution-phase amide condensation reaction, as described in previous publications.[21,22] To construct the branched scaffold of the TD, N-terminal-protected lysine was utilized with HOBt and DIC as coupling reagents. The peptide coupling reactions were conducted in DMF with a 3-fold excess of building blocks and coupling reagents, and the Kaiser test was used to confirm the completion of coupling reactions. Fmoc-protecting groups were removed with 20% (v/v) 4-methylpiperidine in DMF for 30 min. Dde-protecting groups were deprotected in 2% hydrazine DMF solution for 5 min and repeated three times. Boc- and Pbf- protecting groups were removed in TFA/DCM (50/50, v/v) for 30 min. Double bonds were introduced into the TD through a reaction between acryloyl chloride and primary amine with TEA as an acid-scavenging agent. All polymer products were harvested and purified by repeated precipitation with chilled ethyl ether, washed twice, and then dried under vacuum. The resulting TDs were further purified by dialysis (molecular cutoff ~3.5kDa) against deionized water for 2 days with frequent refresh water three times a day and then dried via lyophilization. The structure of the TDs and intermediates were confirmed by ^{1}H NMR and MALDI-TOF MS (**Fig.** S2&3).

Synthesis of disulfide crosslinker N, N'-bis (acryloyl) cystamine (BAC). To synthesize BAC, cystamine dihydrochloride (1 g, 4.44 mmol) was dissolved in 20 mL distilled water. NaOH (10 M, 2 mL) and acryloyl chloride (1.2 g, 13.32 mmol, 10 mL DCM) were added dropwise

simultaneously under vigorous stirring at 0 °C. The solution was then kept at room temperature overnight. The resulting precipitate was extracted three times with 100 mL of DCM and washed three times with 20 mL of distilled water. Finally, BAC was recrystallized from ethyl acetate and dried under vacuum. The ^{1}H and ^{13}C NMR spectra of BAC in DMSO-d_6 are presented in **Figure S1**. ^{1}H NMR (600 MHz, DMSO-d_6) δ 8.37 (t, J = 5.7 Hz, 2H), 6.28 (dd, J = 17.1, 10.2 Hz, 2H), 6.15 (dd, J = 17.1, 2.2 Hz, 2H), 5.66 (dd, J = 10.2, 2.2 Hz, 2H), 3.48 (q, J = 6.4 Hz, 4H), 2.88 (t, J = 6.8 Hz, 4H). ^{13}C NMR (151 MHz, DMSO) δ 165.22, 132.06, 125.83, 38.41, 37.56. TLC-MS (ESI, Advion): Exact mass calc. for C16H19O4S [M+Na]: 283.05, found 283.2.

Synthesis of nanogel. To synthesize the nanogel, a two-neck round-bottom flask was used to dissolve TEGMMA (100 mg, 0.43 mmol), TD, and BAC (4.48 mg, 0.017 mmol, pre-dissolved in 200 µL methanol) in 10 mL of DI water. The mixture was purged with nitrogen for 30 min at room temperature, with stirring at 500 rpm, before being heated to 70 °C. Next, an aqueous solution of KPS (1.16 mg, 0.0043 mmol, 100 µL) was added to initiate the reaction. The reaction proceeded for 1 h under nitrogen protection at 70 °C and was then stopped by cooling the product to room temperature. To remove any unreacted TD and monomer, the nanogel was purified twice by ultracentrifugation (50,000 rpm, 30 min, 15 °C). The resulting particle pellet was resuspended in 10 mL of DI water and transferred into a pre-washed dialysis tube with a molecular cutoff of ~3.5kDa. The nanogel was dialyzed for 2 days. The same procedure was applied to prepare the nondegradable nanogel (NG-BIS) using BIS (2.66 g, 0.017 mmol) instead of BAC as a crosslinker.

Redox degradation of nanogel. To investigate the redox sensitivity of the BAC-containing nanogel (NG-BAC), the NG was incubated at 37°C in PBS (pH 7.2) with TCEP (10 mM) and 2-iodoacetamide (10 mM) or GSH (10 mM). The undegradable NG-BIS were incubated with TCEP (10 mM) as comparison. The hydrodynamic diameter of the nanogel was measured at specific time points using dynamic light scattering (DLS, Zetasizer Ultra, Malvern) to track changes in size. The morphology of the nanogel before and after treatment with the reductant was observed using transmission electron microscopy (TEM, JEM-1400) with uranyl acetate staining.

Agarose gel electrophoresis assays. To determine the loading capacities of the nanogel for LPS or α-LA, an electrophoresis assay was conducted. In this particular assay, the nanogel and LPS/α-LA were pre-incubated in either PBS or a 50% FBS solution for 2 h at different mass ratios. After the pre-incubation step, the samples were mixed with 30% glycerol, which is typically used to help the samples sink into the wells of the gel. The samples were then loaded onto a 1.5% agarose gel in Tris-acetate-EDTA (TAE) buffer. The gel was then subjected to electrophoresis at a constant current of 45 mA for 30 min. After electrophoresis, the gel was imaged using a Bio-Rad Universal Hood II Imager.

Hemocompatibility assay. This study was conducted in accordance with ethical guidelines and protocols approved by the Institutional Review Board of SUNY Upstate (IRB # 754811). The aim of the study was to assess the potential hemolytic effects of nanogel solutions on human red blood cells (RBCs). Fresh human blood (1 mL) was collected from healthy volunteers and mixed with 5 mL of 20 mM EDTA PBS. The red blood cells (RBCs) were then separated by centrifugation at 3,000 rpm for 10 min, washed three times with 10 mL of PBS, and suspended in 20 mL of PBS. Next, 120 μL of the RBC solution was gently mixed with nanogel solutions at final concentrations of 10, 100, 500, and 1000 μg/mL, followed by incubation at 37 °C for 0.5, 4, and 24 h. Positive and negative controls, consisting of Triton-100 (2%) and PBS, respectively, were also included. After incubation, the mixtures were centrifuged at 3,000 rpm for 3 min, and the supernatant was collected to measure hemoglobin concentration by UV-Vis absorbance at 540 nm using a NanoDrop 2000c spectrophotometer (Thermo Scientific). The percentage of hemolysis of the RBCs was calculated using the following formula: Hemolysis% = (OD_{sample} - OD_{PBS}) / (OD_{triton} - OD_{PBS}) × 100%.

Cell culture and MTS assay. RAW 264.7 murine macrophage-like cells, THP-1 human monocytic cells, and HFF-1 human fibroblast cells were obtained from American Type Culture Collection (Manassas, VA). RAW 264.7 and HFF-1 cells were cultured in DMEM medium while THP-1 cells were cultured in RPMI 1640 medium, both supplemented with 10% fetal

bovine serum (FBS), 100 U/mL penicillin G, and 100 mg/mL streptomycin at 37 °C in a humidified incubator with 5% CO_2. Cells were seeded into 96-well plates at a density of 3×10^3 (RAW 264.7, HFF-1) and 8×10^3 (THP-1) cells per well. After overnight incubation, nanogels with varying dilutions were added to each well. Following 72 h incubation, the CellTiter 96 AQueous MTS reagent was added to each well. The cell viability was determined by measuring the absorbance at 490 nm using a microplate reader (BioTek Synergy H1), with untreated cells serving as negative controls. Results were reported as the average cell viability [$(OD_{treat} - OD_{blank}) / (OD_{control} - OD_{blank}) \times 100\%$] of triplicate wells.

Cellular uptake of nanogels by macrophages. Raw 264.7 cells (1×10^4 cells/well) were seeded with DMEM medium overnight in 96-well plates. FITC-α-LA was incubated with TD (mass ratio 1:5), nanogel (mass ratio 1:50), or PEI (mass ratio 1:2) for 30 min and added to the cell culture medium at a final concentration of 5 μg/mL FITC-α-LA. After a 2 h incubation, the cell culture medium was removed, and the cells were washed three times with cold PBS and fixed with 4% paraformaldehyde for 10 min. The cell nuclei were stained with 4',6-diamidino-2-phenylindole (DAPI). Finally, fluorescence microscopy was used to image the cells.

LPS attenuation *in vitro.* To assess the effect of nanogels for LPS attenuation, Raw 264.7 cells were seeded in 96-well plates at a density of 2×10^4 cells/well. The LPS stock solution (50 μg/mL) was either pretreated with different mass ratios of nanogels/PMB/TD overnight or added separately (nanogel, then LPS) to the cell culture medium. As a control for cytokine production comparison, the untreated LPS stock solution was directly added to the cell culture to achieve a final LPS concentration of 50 ng/mL. After overnight incubation, the cell medium was collected, and the supernatant was obtained through centrifugation. The levels of TNF-α and IL-6 production were measured using a commercial ELISA Kit.

Experimental animals. The experimental procedures involving mice were conducted in accordance with the AAALAC (Association for Assessment and Accreditation of Laboratory Animal Care) guidelines and were approved by the Committee for the Humane Use of Animals

of State University of New York Upstate Medical University (IACUC # 437). C57BL/6 wild type mice (6-8 weeks old, obtained from Charles River, USA) were maintained under pathogen-free conditions with 22 ± 2 °C temperature, 60% air humidity, and 12 h light/dark cycle. The mice were allowed to acclimatize for at least 4 days prior to the experiments. The NF-κB reporter HLL (HIV-long terminal repeat/luciferase) mice colony was maintained in our laboratory by crossing hemizygous mice with their wildtype siblings or with C57BL/6J. The genotype of the offspring was confirmed by the presence of NF-κB-induced bioluminescence after injection of luciferin (200 µL/20 g mice, 150 mg/kg) at 3-4 weeks of age. 8-12 week-old HLL mice were used for *in vivo* bioluminescence studies.

Pharmacokinetics (PK) and biodistribution Study. To investigate the blood circulation of nanogel, Rhodamine B (RB) labeled nanogel was used in a study involving wild type mice (n=3-4 per group). The nanogel was synthesized using TD containing RB ($PEG^{5k}RB_2$) and was i.v. injected into the mice at a dose of 50 mg/kg. For comparison, the TD $PEG^{5k}RB_2$ was also injected intravenously with an equivalent amount of RB in nanogel (the concentrations were quantified by fluorescent signal). At predetermined time points after injection, blood samples were collected from the tail vein and plasma was separated by centrifugation (7000 rpm, 5 min) for quantitative measurement. The fluorescent signal of RB was recorded at an excitation/emission of 525/580 nm using a fluorescence microplate reader (Synergy H1, BioTek Instruments Inc., Winooski, VT). After 28 h, the mice were sacrificed, and their organs were harvested and homogenized with 2x PBS. The supernatant was then collected by centrifugation at 10,000 rpm for 5 min, and the fluorescent signal was recorded using the same fluorescence microplate reader.

LPS attenuation *in vivo*. Randomization was performed to assign wild type mice into different treatment groups (n = 3-5). For NG treatment after LPS i.v. injection, mice received an i.v. injection of LPS at a concentration of 0.1 mg/kg. 5 min after LPS injection, the animals were injected with either PBS or NG at a dose of 50 mg/kg via i.v.. For NG treatment before injection of LPS, mice were given an i.v. injection of either PBS or NG at a dose of 50 mg/kg. After 5 min, LPS was injected intravenously at a dose of 0.1 mg/kg. Blood samples were collected from the

tail vein at 2 h and 4 h after LPS injection, and plasma was separated by centrifugation at 7000 rpm for 5 min for subsequent ELISA measurement.

Real-time *in vivo* imaging of mice after LPS injection. *In vivo* bioluminescence studies were conducted on NF-κB reporter HLL mice. To establish the basal bioluminescence level, luciferin solution was injected i.p., and after 10 min, the abdominal bioluminescence was acquired using an *in vivo* imaging system (Ami-HTX) while the mice were anesthetized with isoflurane. On the day of the experiment, LPS was injected i.v. at a dose of 0.1 mg/kg. The nanogel (50 mg/kg) was i.v. injected into mice either 5 min before or after the LPS injection. Control groups were injected with PBS, nanogel (50 mg/kg) or LPS (0.1 mg/kg) in PBS solution. The abdominal bioluminescence signals were acquired using Ami-HTX (Spectral Instruments Imaging) at 2 h, 4 h, 6 h, 24 h and 48 h post injection.

Cytokines removal from biological fluids. In this study, RAW 264.7 cells were seeded in 96-well plates at a density of 2×10^4 cells per well. LPS stock solution was added directly to the cell culture to achieve a final LPS concentration of 50 ng/mL. After 24 h of co-incubation, the cell culture medium was collected. Septic mice were induced by the cecal ligation and puncture (CLP) procedure as previously described. 24 h after CLP, plasma and peritoneal lavage samples were collected from the septic mice for cytokine removal analysis. Blood samples were obtained from surgical sepsis patients in EDTA tubes and de-identified for this study under a protocol approved by the SUNY Upstate Institutional Review Board (IRB #1321635-7). Plasma was isolated for incubation with nanogel. To evaluate nanogel binding with cytokines, 100 μL of nanogel samples were mixed with pure IL-6, TNF-α, or IL-1β at different mass ratios and incubated at 37 °C overnight. After incubation, cytokine concentrations were quantified using ELISA. The cytokine removal efficacy of nanogel was tested by adding different concentrations of nanogel into LPS-challenged cell culture medium, sepsis mice plasma and peritoneal lavage, and sepsis human patient plasma, respectively. After overnight incubation at 37 °C, cytokine levels were measured by ELISA from the cell culture medium, plasma, and peritoneal lavage samples. All experiments were performed in triplicate.

Sepsis model induced by CLP in mice. The mice were anesthetized using intraperitoneal ketamine/xylazine injection and a midline incision was made in the lower quadrants of the abdomen after disinfecting the surgical area. The cecum was then located, ligated, and perforated with a 22-gauge needle at two sites. A small amount of feces was extruded by gently squeezing the cecum, and it was returned to the peritoneal cavity before the incision was closed. In the sham group, the same procedure was followed without the CLP procedure. The mice were resuscitated with saline and kept under observation with free access to food and water. Buprenorphine was administered for postoperative pain relief. After the standard CLP procedure, mice were randomly assigned to receive nanogel (50 mg/kg) or saline for five doses over five days. The animals were monitored for mortality, body weight, and temperature for 14 days. The study included two groups with 8-10 mice each.

Cytokine analysis and histological examination. The mice underwent the same CLP procedure, with one group treated with nanogel (at a dose of 50 mg/kg) and another group treated with saline as a control. A sham group was also included, where the cecum was taken out and put back before wound closure. 24 h after the CLP procedure, about 100 μL of blood was collected from the tail vein and plasma was separated for cytokine analysis using ELISA. At the end of the study (14 days), the mice were sacrificed under anesthesia and their heart, liver, kidney, spleen, and intestine were harvested. The tissue was frozen in OCT cryo-embedding medium for histological analysis. For pulmonary structure-function analysis, the right-side lung lobe was fixed by infusing formalin into the cannulated main bronchus and then immersed in a container of formalin for at least 24 h. The fixed lung tissue was embedded in paraffin. All the organs were sectioned (5 μm) and stained with hematoxylin and eosin (H&E) for histopathology analysis.

Statistical analysis. All data points referred to the mean ± standard deviation (SD) and were based on at least three separate experiments (n=3). All statistical tests were performed by GraphPad Prism using one-way analyses of variance (ANOVAs) for two-group and multiple-

group analyses. Statistical significance was represented as *: $p<0.05$; **: $p<0.01$; ***: $p<0.001$; ****: $p< 0.0001$.

Results

Synthesis and Characterization of TD-NG

The lipid A is the most immunogenic segment in lipopolysaccharide (LPS). It possess two negative charge groups and hydrophobic lipid moieties,[23] which could be neutralized and sequestered with molecules containing positively charge and hydrophobic groups, e.g., polymyxin B. In our previous study, we developed a well-defined linear-dendritic telodendrimer (TD) nanoplatform enable customized nanocarrier design and optimization for both drug and protein delivery.[24] We conjugated the protein-binding TD into the core-shell PNIPAM/PMPC nanogel (NG), which showing selective adsorption of LPS and proinflammatory cytokines.[17] The two stepwise polymerization process is challenging for reproducibility for surface shell coating efficiency of the core-shell nanogel synthesis. PNIPAM based nanogel shows significant cytotoxicity and hemolytic activity at 500 ug/mL in cell culture. In addition, the solubility of the polymerizable dendritic TD domain poses the challenges for TD-NG synthesis. Alternatively, we designed a new version of PEGylated TD NT NG via a one-port precipitation polymerization with biocompatible monomers and biodegradable crosslinker (**Fig. 1a**) for systemic injection and selective adsorption of LPS and cytokines for the sepsis treatment (**Fig. 1b**).

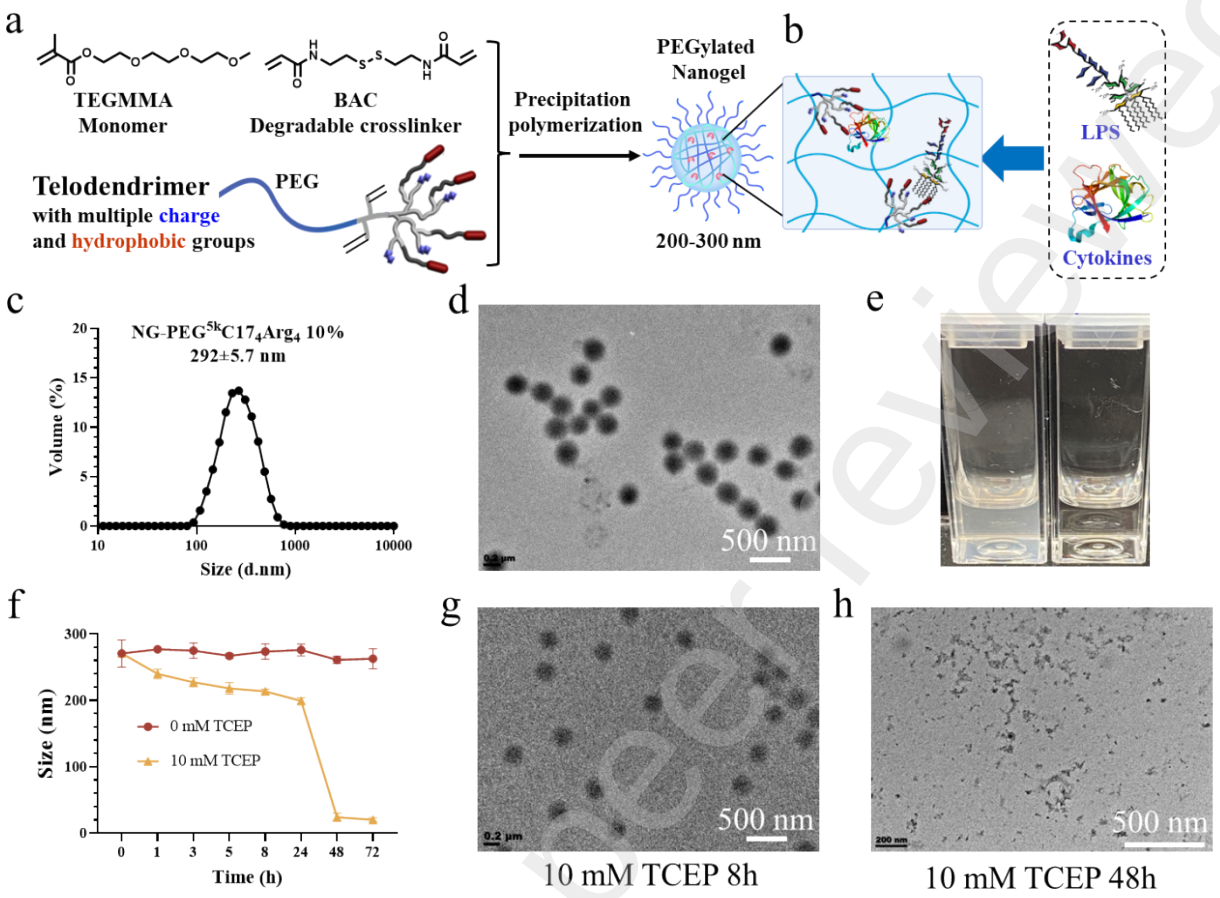

Figure 1. (a) Schematic representation of the synthesis of PEGylated nanogel (NG) with the polymerizable telodendrimer (TD) and biocompatible thermo-sensitive ethylene glycol monomer (TEGMMA) and degradable disulfide linker (BAC); and (b) illustration of selective LPS and cytokine removal by TD-NG; (c) hydrodynamic sizes and (d) the morphology of nanogel with 10% $PEG^{5k}C17_4Arg_4$ measured by DLS and TEM; (e) degradable nanogel (NG-BAC) solution before (left) and after (right) incubated with 10 mM TCEP for 48 h; (f) the size of the nanogels NG-BAC without or with 10mM TCEP; TEM micrographs of NG-BAC after (g) 8 h and (h) 48 h incubation with 10mM DTT (the data are presented as mean ± SD, n = 3; TEM scale bar: 500 nm).

In order to improve the biocompatibility of nanogel, we apply commercially available triethyleneglycol methyl ether methacrylate (TEGMMA) as monomer, and we prepared a biodegradable disulfide bond-containing crosslinker (N, N'-Bis(acryloyl)cystamine (BAC)) for

nanogel preparation. The chemical structure of BAC crosslinker was confirmed and characterized by both carbon and proton NMR and MS (**Fig. S1**). As comparison, non-degradable commercially available crosslinker (N, N'-methylenebis(acrylamide), BIS) was also applied for nanogel synthesis for comparison. We first introduce polymerizable double bonds in the TD at the adjacent site between the linear PEG and the protein/LPS binding dendron, in order to anneal the functional TD NT into NG via one-pot precipitation polymerization. The presence of PEG in TD increases the solubility and allows for the integration larger dendritic cluster of charge/hydrophobic combination than our previous core-shell TD nanogel system[17] to increase the affinity for biomacromolecules capture. The dendritic domain possesses four C17 fatty acid tails and different charges (**Fig. 1a** and **Table 1)** can be introduced in TD NT NG according to our previous studies for effective bioscavenging.[15] The TD and intermediates have been characterized by MALDI-TOF MS and the proton NMR as shown in **Figure S2** and **S3**. During the precipitation polymerization, TDs can be polymerized into the hydrogel network and PEG chains displays on the surface of nanogel to increase the stability of nanoprecipitate, as evidenced by the reduced particle sizes (200-300 nm) than nanogels without PEGylated TD (~360 nm) (**Table 1**). In addition, the PEGylated nanogel remains and only slightly reduces the particle sizes when temperature increased, as the thermosensitive poly(TEGMMA) becomes more hydrophobic and cause the core of nanogel shrink slightly (**Fig. S4**). The particle sizes remain about ~200 nm at body temperature of 37 ^{o}C. While, the bare poly(TEGMMA) NG forms large aggregates and precipitate at the body temperature after purification (**Fig. S4**).

We also prepared the rhodamine B (RB)-labeled telodendrimer (RB-TD) to test the efficiency of chemical immobilization of TD in NG by monitoring the release profiles of RB-TD from NG via fluorescent measurements **(Fig. S5)**. RB-TD with or without polymerizable double bonds were prepared for comparison. As shown in **Figure S5c&d**, free RB-TD has particle size of 15 nm and RB-TD NG has particle size around 230 nm. The RB-TD without double bonds only has 38% yield of incorporation into nanogel. While the polymerizable RB-TD has high conversion yield of 89% and ~100% into nanogel with 2% and 4% crosslinking degree (**Fig. S5e)**. RB-TD without double bonds showed a fast release from nanogel with ~40% release after 48 h, owing to the physical entrapment of TDs in the crosslinking nanogel network. Polymerizable TD instead significantly decreases the rate of leakage from NG, which is further inhibited by the increased

crosslinking degree from 2% to 4% (**Fig. S5f**). Based on this result, we made nanogels using TDs with double bonds and 4% crosslinking degree for further study.

Nanogels were monodispersed in sizes, with an average diameter of 200-400 nm in phosphate-buffered saline (PBS) (**Table 1** and **Fig. 1c** and **S6**). TEM micrographs showed that the nanogels maintained a uniform spherical morphology and homogeneous size distribution (**Fig. 1d**). The TD ($PEG^{5k}C17_4Arg_4$) nanotrap with arginine (Arg) showed significant positive charge (zeta-potential: 30.7±0.6 mV, **Table S1**) in aqueous solution. After conjugated in the nanogel, at the TD ratio less than 10%, the resulting NGs showed neutral surface (**Table 1**), due to the PEG surface coating. With the increasing ratio of TD to 15% and 20%, the NGs exhibited slightly positive surface with zeta-potential 3.4±0.3 and 3.5±0.07 mV, respectively, which may cause nonspecific adsorption and are not preferred for *in vivo* application. We also prepared TDs with negatively charged oxalic acid (OA) and succinic acid (SA) for comparison. These TDs display strong negative surface charges with zeta potentials about -20 mV (**Table S1**), which are however sheltered efficiently by PEG in 10% TD-NGs, exhibiting close to neutral charges (**Table 1**).

Table 1. TD composition, size, PDI, zeta-potential and LPS-capturing capacity of NGs.

Entry	TD (Feed ratio wt%)	Size (d. nm)	PDI	Zeta potential (mV)	LPS-capturing capacity
1	Blank	361±3	0.03±0.04	-0.4±0.1	---
2	PEG^{5k}-$C17_4Arg_4$(5%)	321±10	0.02±0.01	-0.7±0.08	<1%
3	PEG^{5k}-$C17_4Arg_4$(7.5%)	202±0.8	0.4±0.01	0.0±0.4	1%
4	PEG^{5k}-$C17_4Arg_4$(10%)	266±22	0.2±0.04	-0.7±0.2	4%
5	PEG^{5k}-$C17_4Arg_4$(15%)	226±17	0.2±0.007	3.4±0.3	4%
6	PEG^{5k}-$C17_4Arg_4$(20%)	246±7	0.1±0.03	3.5±0.07	4%
7	PEG^{5k}-$C17_4SA_4$(10%)	256±5	0.1±0.03	-0.7±0.1	---
8	PEG^{5k}-$C17_4OA_4$(10%)	348±10	0.06±0.05	-1.5±0.9	---

The TD structures can be found in **Figure S3**. Data are represented as means ± SD, n = 3.

Biodegradation of NG

The incorporation of disulfide crosslinker BAC into nanogel enables the particle biodegradation triggered by reducing reagents *in vivo*, e.g., glutathione (GSH).[25] The response of BAC containing nanogel (NG-BAC) to the reducing agents was evaluated by monitoring their particle

size changes with the incubation with GSH or tris(2-carboxyethyl)phosphine (TCEP). The nanogel with undegradable crosslinker BIS (NG-BIS) were also incubated with reductant as a control. In the presence of 10 mM TCEP, the NG-BIS remains its size and morphology even after 72 h incubation (**Fig**. **S7a-c**). In comparison, the size of NG-BAC decreased from 285 ± 10 to 245 ± 4 nm after 1 h incubation with 10 mM GSH at 37 °C (**Fig**. **S7d-f**). At 24 h, the size of NG-BAC increased to around 400 nm, which was also evidenced in the TEM images revealing swollen and larger particle sizes. It may be due to the negative charges of glutathione increase the polarity and charge interactions with the arginine group in TD as extra physical crosslinking, resulting in the nanogel swollen but still intact nanoparticles. To further test this hypothesis, we apply TCEP and 2-iodoacetamide into the nanogel solutions. The 2-iodoacetamide can react with newly formed thiol group and effectively break the polymer chain crosslinking. The sizes of the NG-BAC are gradually decreased when treated with TCEP and 2-iodoacetamide from 266 nm to 214 nm and 24 nm after 8 h and 48 h incubation, respectively, monitored by DLS (**Fig. 1f**). In the absence of a reductant, the nanogel maintained its stability in an aqueous solution and displayed a milky color, with an approximate size of 300 nm. Images in **Figure 1e** reveals the disappearance of nanogels in solution before (left) and after (right) the incubation with TCEP for 48 hours, which was also confirmed by TEM images: 197±21 nm observed after 8 h and only fragmented pieces left after 48 h incubation with TCEP (**Fig. 1g&h**).

The Scavenging of LPS and Proinflammatory Cytokines by TD-NG

According to our previous study, the TD can be freely customized by different functional groups for efficient protein encapsulation through synergistic combination of multiple hydrophobic and charge interactions. Here, we construct TD with hydrophobic C17 and different charged groups, e.g., Arg, OA or SA for the LPS and proinflammatory cytokines capturing. From the agarose gel electrophoresis (**Fig. S8a**), the TD possessing positively charged arginine groups show efficient capture for the negatively charged LPS. As expected, the nanogel with negatively charged TD (OA and SA) didn't exhibit any scavenge capability to LPS (**Fig. S9**). Similarly, the blank nanogel without TD moieties didn't exhibit any effective capture of LPS (**Fig. S8b**). Then, we further tested the capacity of NG with different $PEG^{5k}C17_4Arg_4$ density for LPS-capturing by agarose gel electrophoresis. As shown in **Table 1** and **Figure S10**, the NG-5% TD only partially

captures LPS at a high NG/LPS ratio of 100/1 in mass. While NG-7.5% TD can completely absorb the LPS at 100/1 ratio, correspondingly equal to a capacity of 1% in mass. With the increased TD content in NG to 10%, the LPS capturing capacity can be increased to 4%. However, further increase of TD content to 15% and 20% didn't further increase the capturing capacity, which may be due to the increased TD aggregation in NG resulting in the hindered molecular diffusion. In addition, these NG with 15-20% TD show slightly positive surface charges (**Table 1**); thus TD-NG (10% $PEG^{5k}C17_4Arg_4$) was selected for further test in LPS and cytokine adsorption.

A negatively charged medium-sized model protein, α-LA (Mw 14 kDa, PI 4-5), was selected to mimic proinflammatory cytokines in TD-NG scavenging assay. As shown in agarose electrophoresis (**Fig. S11)**, TD-NG (10% $PEG^{5k}C17_4Arg_4$) effectively traps the fluorescently labeled α-LA at a 25/1 ratio of NG/α-LA in mass in the presence of excess of 200-fold BSA. We then further confirm the loading capacity of LPS and α-LA in TD-NG (10% $PEG^{5k}C17_4Arg_4$) quantitatively by ultracentrifugation method. The NG were preincubated with different ratio of FITC-LPS or RB-α-LA for 2 h. Then the samples were centrifuged (50,000 rpm, 1 h, 15 ºC) to separate the supernatants for the fluorescent determination of the free LPS or protein concentration. As shown in **Figure 2a**, more than 94% of LPS and α-LA can be captured at a 25/1 ratio of NG to LPS or α-LA in mass, which is consistent with the agarose gel results (**Fig. S10 and S11**).

Most proinflammatory cytokines (TNF-α, IL-1, IL-6, IL-12, and HMGB-1) have negative charges with PIs ranging between 4.1 and 6.4.[11] In order to determine the cytokine absorption property of NG, we co-incubated TD-NG (10% $PEG^{5k}C17_4Arg_4$) with proinflammatory cytokines (TNF-α, IL-6 and IL-1β) at different mass ratio at 37 °C for overnight and then test the free cytokines level by ELISA. As shown in **Figure 2b**, around 86%, 97% and 69% of TNF-α, IL-6 and IL-1β can be removed at a feeding ratio of 400/1 in mass of NG to cytokines at their pathological plasma concentrations, which indicated the potential of efficacy of TD-NG for *in vivo* endotoxin and pro-inflammatory cytokines absorption for sepsis treatment.

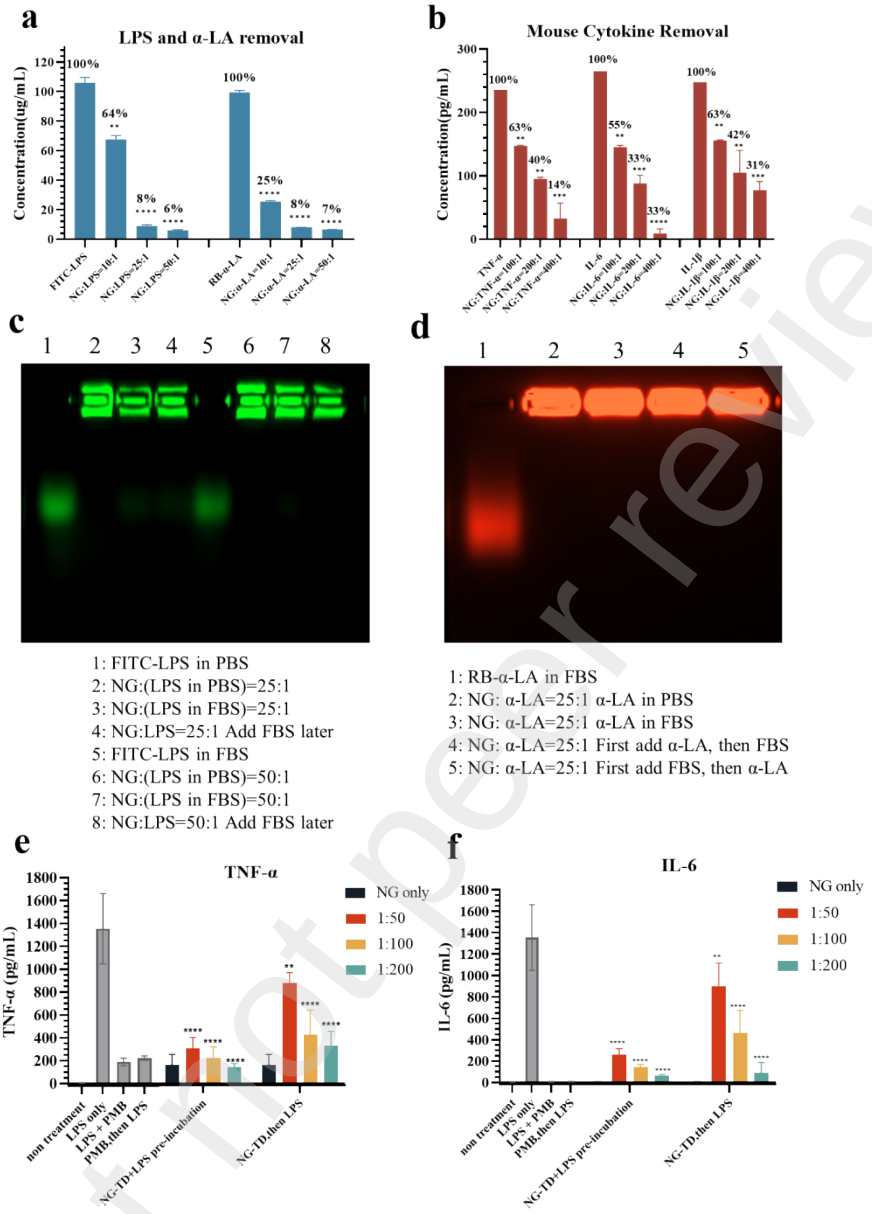

Figure 2. The removal of (a) FITC-LPS and RB-α-LA and (b) pro-inflammatory cytokines (TNF-α, IL-6 and IL-1β) by TD-NG (10% $PEG^{5k}C17_4Arg_4$) after incubation at different mass ratio at 37 °C for overnight; Agarose gel electrophoresis profiles of the TD-NG for FITC-LPS (c) and RB-α-LA (d) loading in the presence of 50% FBS solution at the 25/1 and 50/1 mass ratio ; cytokines level of (e) TNF-α and (f) IL-6 in RAW 264.7 cell culture medium with overnight stimulation with LPS (50 ng/mL), LPS/PMB (1/20 mass ratio) or LPS/TD-NG (10% $PEG^{5k}C17_4Arg_4$) (preincubated for overnight or added separately at LPS/NG mass ratios 1/50, 1/100, 1/200), respectively. (n = 3, mean ± SD).

To exam the capability of the NG for LPS-scavenging in biofluid, LPS was doped into the fetal bovine serum (FBS, 50%) solution and then incubated with NG. Even though plenty of proteins exist in FBS solution, the nanogel remains effective for selective LPS capture via size-exclusive effects and multivalent TD affinity. From the agarose gel result, the LPS can be completely removed from FBS solution at 25 to 1 mass ratio of NG to LPS (**Fig. 2c**, lane 3, 7). We also tried to first incubate the NG and LPS, then FBS was added (lane 4, 8), which didn't influence the captured LPS (**Fig. 2c**). Similarly, α-LA can be completely captured by NG at 25/1 mass ratio both in PBS and FBS as co-incubation or sequential incubations, **(Fig. 2d**) indicating potential effective and selective cytokine adsorption from blood.

LPS attenuation from immune stimulation

LPS activates Toll-like-receptor 4 (TLR4), which induces the production of inflammatory mediators (e.g., TNF-α and IL-6) and triggers cytokine storm. The dysregulated cytokine release aggravates the sepsis development and progress. So, we first test whether TD-NG can attenuate LPS from immune stimulation. LPS was incubated with TD-NG and then added into culture medium of RAW 264.7 macrophage cells. After overnight incubation, cell culture medium was collected for the TNF-α and IL-6 production analysis. The free LPS stimulation was used as positive control and Polymyxin B (PMB), a cationic LPS-neutralizing antibiotic, was used as comparison. As expected, TNF-α and IL-6 productions were significantly increased by free LPS-stimulation. As expected, it can be effectively attenuated by PMB (**Fig. 2e&f**). The blank NG didn't induce cytokine production. NG showed a dose dependent LPS attenuation in reducing the cytokines production by macrophages. To mimic clinical disease treatment, we added LPS and nanogel separately into the cell culture medium to further determine if NG can bind LPS in situ to inhibit cytokine production for inflammation control. As shown in **Figure 2e** and **2f**, even though the inhibition were slightly reduced in comparison to the preincubation, NG can still effectively attenuate the LPS-induced proinflammatory cytokines production at high NG/LPS ratios of 100/1 and 200/1, which is applicable for *in vivo* sepsis treatment given the low LPS concentration in sepsis patients below ng/mL level.[26]

Cytokine Removal from Biological Fluids

The management of hyperinflammation is crucial for the treatment of sepsis. Based on the *in vitro* results, we expect that the TD-NG may be able to sequester proinflammatory cytokines from biofluids and blood thus to blocks sepsis cascade. We collected cytokine-containing biological fluids, including LPS-stimulated RAW264.7 cell culture medium, plasma and peritoneal lavage from septic mice and plasma from human sepsis patients for incubation with NG *in vitro* for cytokine adsorption analysis. As shown in **Figure 3a**, LPS stimulation significantly induced the production of cytokines in the cell culture medium, e.g., TNF-α and IL-6. The NG with positively charged TD ($PEG^{5k}Arg_4C17_4$) nanotrap can effectively adsorb both TNF-α and IL-6 with a dose dependent manner after overnight incubation. In contrast, TD only or nanogel with negative charge ($PEG^{5k}OA_4C17_4$ and $PEG^{5k}SA_4C17_4$) didn't show any capacity for TNF-α and IL-6 adsorptions (**Fig**. **S12**). We also collected the plasma and peritoneal lavage fluid from LPS-induced septic mice, and incubated with different concentrations of NG. TNF-α and IL-6 level in the fluids were analyzed by ELISA. Similarly, TD-NG can scavenge those proinflammatory cytokines level in a dose-dependent manner (**Fig. 3b&c**). Further, plasma from clinical patients with severe sepsis were collected for nanogel incubation. TNF-α is an early proinflammatory cytokine and detected to be low in severe patient; While IL-6 can be accumulated to high ng/mL level in patient blood, which can be decreased significantly more than 95% after incubation with NG (**Fig**. **3d**).

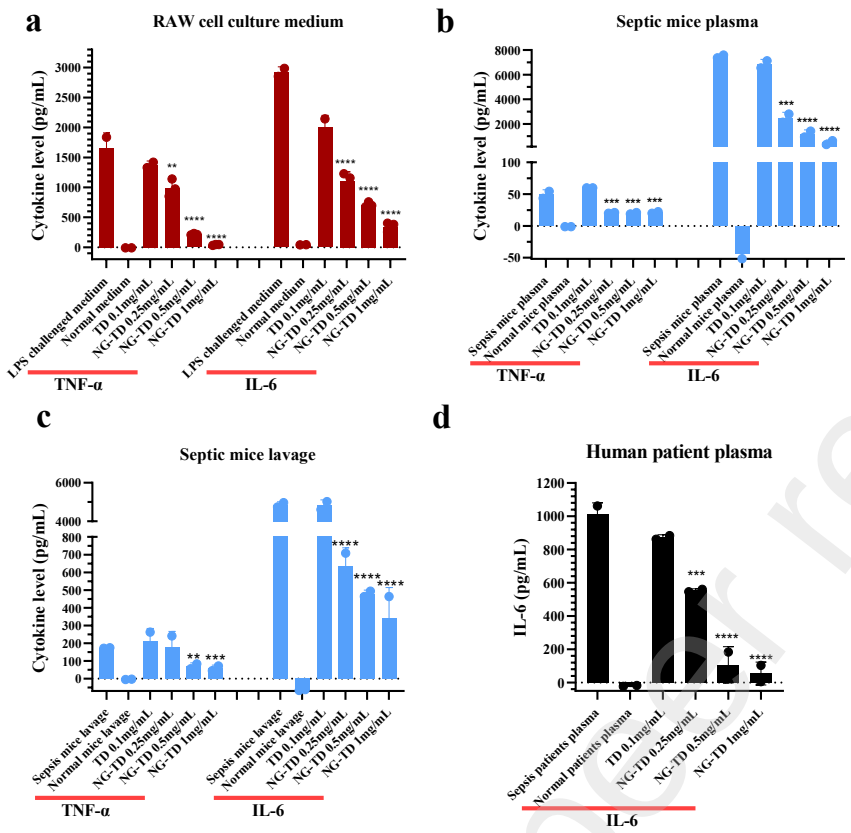

Figure 3. The management of hyperinflammation with TD-NG *in vitro*. The removal of cytokines TNF-α and IL-6 by TD-NG in compare with the TD in (a) RAW 264.7 cell culture medium after LPS stimulation (50 ng/mL) for 24 h; (b) sepsis mice plasma and (c) peritoneal lavage collected from mice 24 h after the CLP surgery; (d) human patient plasma (n = 3, mean ± SD).

TD-NG toxicity and cellular uptake

The *in vitro* cytotoxicity of NGs was tested in cell culture and measured by MTS assay. TD-NG is not cytotoxic to both immune cell lines (RAW 264.7 and THP-1 cells) and normal cell line (HFF-1 cells) up to 2 mg/mL after 72 h incubation (**Fig. 4a**). In addition, NGs were incubated with red blood cells in the concentration range of 10-1000 μg/mL for 24 h. The NGs barely show any hemolysis even at the highest concentration 1000 μg/mL (**Fig. 4b**).

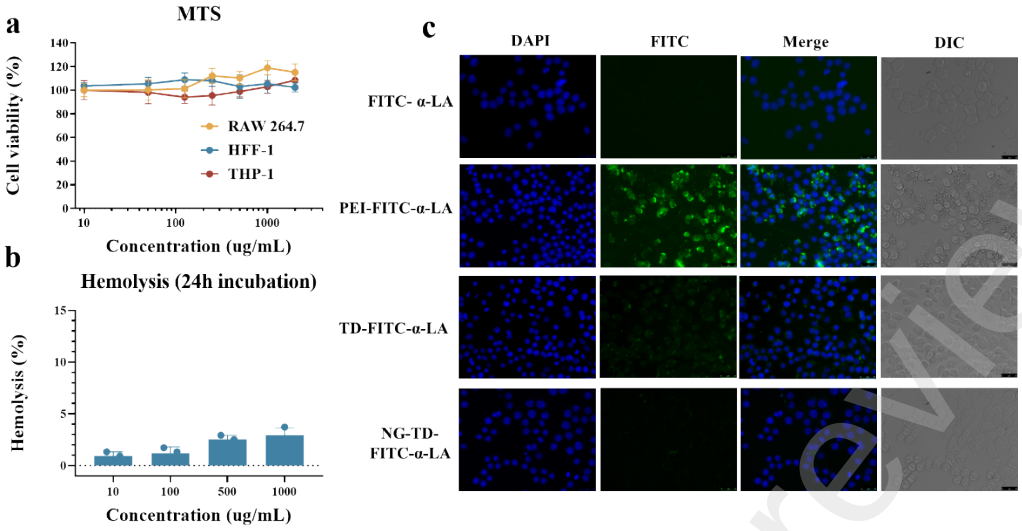

Figure 4. (a) Cell viability assays on RAW 264.7, HFF-1 and THP-1 cells after 72 h incubation with the TD-NG as measured by MTS assay; (b) hemolytic property at 24 h after the red blood cell suspension was mixed with the TD-NG at different concentrations; (c) the fluorescent microscopic images of RAW 264.7 cells after incubation with the PEI, TD, TD-NG encapsulated FITC-α-LA at a concentration of 5 μg/mL of α-LA for 30 min at 37 °C: cell nucleus was stained into blue with DAPI, green color is FITC-α-LA. Scale bar: 25 μm.

As nanotrap is designed to scavenge the circulating septic molecules, low phagocytosis of nanogel is preferred to ensure long circulation for effective immune modulation. It has been demonstrated that nanoparticles with antifouling PEG chain on the surface have long circulation time in human blood with the reduced nonspecific uptake by macrophages. Immune cell uptake was evaluated in cell culture with murine macrophage RAW 264.7 to determine the stealth properties of the TD-NG compared with TD only. The cationic poly(ethylene imine) (PEI) was used as a positive control. NG, TD and PEI were preincubated with FITC-α-LA for 30 min for effective adsorption/complexation as shown in agarose gel electrophoresis (**Fig. S13a**), then added into the cell culture medium (final concentration of α-LA is 5 μg/mL). The cells were fixed, and nuclei were stained with DAPI after 30 min incubation for microscope observation. As shown in **Figure 4c**, the PEI complex was effectively taken up by immune cells, due to the positive charges. The self-assembled TD micelle with Arg groups shows slightly positive surface

charge (**Table S1**), which leaded to mild cell uptake by macrophages. The TD-NG can significantly decrease the cellular uptake due to its neutral PEG surface. The quantitative fluorescent intensity analysis of cell signals reveals even lower cell uptake of TD-NG/FITC-α-LA than free protein FITC-α-LA (**Fig. S13b**).

Pharmacokinetics and biodistribution of NG

The hemocompatibility of NG is important for *in vivo* systemic application. As shown in **Figure 4b**, NG is biocompatible in contact with blood cells without hemolytic properties at the tested concentration of 1 mg/mL. We further characterize the biocompatibility of NG in the presence of endotoxin and plasma proteins to avoid risk of blood clotting by NG aggregation before *in vivo* application. Thus, we incubate TD-NG (10 mg/mL) with or without LPS (25/1 mass ratio) in PBS or 50% mouse plasma and particle sizes was monitored via DLS particle sizer (**Table S2**). NG remains sizes unchanged in plasma with or without LPS (~300 nm). In addition, TEM images of TD-NG after overnight incubation with LPS in both PBS and plasma confirm the absence of any aggregation without changes in particle size (**Fig. S14**). Further, we tested the potential acute *in vivo* toxicity of TD-NG in mice after i.v. injection. We started the dose escalation from 50 mg/kg to 100 mg/kg in wild type B6 mice. As expected, no observable side effects were witnessed after injection as monitored daily, e.g., physical appearance, activity behavior, body temperature, and body weight. However, TD-NG solution becomes more viscous at 10 mg/mL for i.v. injection at a dose level of 100 mg/kg, thus, we keep dose of 50 mg/kg for the following test.

To study the PK profile of NG, we synthesized a Rhodamine B (RB)-decorated polymerizable TD for fluorescent-labeling of NG synthesis (**Fig. S5**). RB-NG (50 mg/kg) was i.v. injected into normal mice through tail vein. The corresponding RB-TD nanoparticle was also administrated as comparison. Blood samples were collected at determined time points for fluorescent analysis (excitation 550 nm, emission 585 nm). Free RB-TD self-assembles into micelle nanoparticle (15 nm) also with PEG surfaces, which also avoids fast phagocytic clearance *in vivo*. As shown in **Figure 5a**, free RB-TD nanoparticles exhibit a sustained circulation in mouse blood with a $t_{1/2\beta}$ of 4.4 h. In comparison, TD-NG sustains a longer blood circulation with a > 4 times of increase in $t_{1/2\alpha}$ and 1.7 times increase in $t_{1/2\beta}$ (7.5 h), and 2.1 times higher in area under curve (AUC) in

comparison with free TD nanoparticle. At 28 h post-injection, the mice were sacrificed for *ex vivo* organ imaging as shown in **Figure 5b**. The majority of signal were detected in GI tract and liver. Further, these major organs and tissue were collected and homogenized with lysis buffer for biodistribution analysis via spectrometry measurement. As shown in **Figure 5c**, significantly higher concentration of fluorescence was observed in feces rather than the cleaned colon and intestine, which indicated that TD-NG can be excreted through the liver bile-duct into feces for elimination.

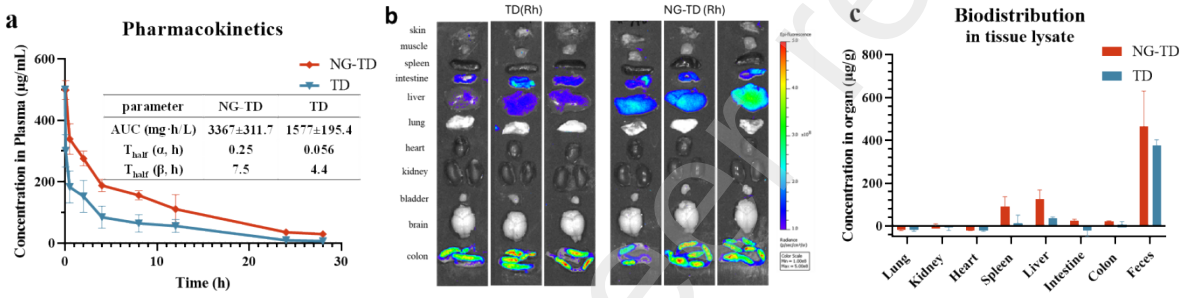

Figure 5. (a) Plasma concentration-time profile of TD-NG (50 mg/kg) and TD after administration as a single dose i.v. injection. AUC (mg·h/L): area under the concentration time curve; $T_{1/2}$ (h): half-life; data are expressed as the mean ± SD (n = 3); (b) *ex vivo* organ imaging of the fluorescent intensity and (c) tissue organ biodistribution of TD determined in tissue lysate via fluorescence spectrometry at 28 h post i.v. injection.

TD-NG modulate LPS-induced inflammatory response *in vivo*

Intravenous injection of LPS in mice induces significant hyperinflammation, such as dysregulated cytokine production, immune cell infiltration and organ dysfunction and failure, eventually causing death. Based on the promising *in vitro* attenuation of LPS and proinflammatory cytokines, we further evaluate TD-NG (Arg) for *in vivo* treatment of sepsis induced by LPS. HIV-LTR/Luciferase (HLL) mouse has a transgene of luciferase reporter for NF-κB activation in inflammatory responses. We create sepsis models in HLL mouse using LPS stimulation to test the immune modulation effects of nanogels. TD-NG (10% $PEG^{5k}C17_4Arg_4$, 50

mg/mL) was injected into mice through tail vein 5 min after LPS i.v. injection (**Fig. 6b**). Mice were i.p. injected of luciferin before imaging at t = 0 h for baseline and at 2, 6, 24 and 48 h after LPS injection to monitor the systemic inflammation via bioluminescent signal. As shown in **Figure 6a**, LPS-treated mice exhibited significant increase in luminescent signal at 2 h and 4 h post injection. However, the signal remained low in mice treated with TD-NG solution following LPS treatment throughout the observation, indicating the attenuated activity of LPS. TD-NG injection alone did not induce any inflammatory signals similar as PBS injection. The quantitative result of the luminescent signal was displayed in **Figure 6c**. LPS treated group showed a peak at 2 h after administration and the NG treatment group maintained low level of bioluminescent signal. These results indicated that the TD-NG can capture LPS in the blood simultaneously and inhibit the NF-κB activation and inflammatory response stimulated by LPS (**Fig. 6d**).

To further confirm the effectiveness of *in vivo* inflammation control, wild type mice were treated with LPS (0.1 mg/mL) via i.v. injection. 5 min later, the mice were treated with either TD-NG or PBS (**Fig. 6e**). Blood was collected from tail vain at 2 h and 4 h after the LPS injection to analyze the plasma cytokine level. TNF-α is an early stage proinflammatory cytokine to initiate inflammation, which peaked at 1 h or 2 h after injection.[27] As shown in **Figure 6f**, the LPS treatment induces high TNF-α production (~270 pg/mL) in plasma 2 h after treatment, which gradually decreased to around 80 pg/mL at 4 h, which is consistent with the luminescent signal results in **Figure 6a**. The nanogel treatment significantly reduced the level of TNF-α at both time points. At 4 h, TNF-α level in the LPS/NG group returned to the level in normal mice. The IL-6 normally peaked at around 3 h or 4 h after LPS stimulation.[28] The IL-6 level in LPS group increased to about 8 ng/mL at 2 h and continuously increased to 10 ng/mL at 4 h post treatment. In contrast, IL-6 in the LPS/NG group was substantially reduced in comparison to LPS group, which is although still significantly higher than normal level, due to the fast on-site of pre-applied LPS for immune stimulation. Importantly, IL-6 in the LPS/NG group decrease at 4 h post-treatment which was five-times lower than that in LPS group and close to normal level. These results indicate that the TD-NG with long blood circulation time can inhibit the of hyperinflammation *in vivo* and stop sepsis perpetuation.

In patients with the high risk to develop sepsis, e.g., septic polytrauma, and severe pneumonia, it may be beneficial to pretreat patient with preventive and passive immune modulation therapy. Thus, we also tested the prophylactic effect of NG to LPS induced inflammation in both HLL mice and wild type B6 mice. The NG/PBS were first injected intravenously followed by the LPS injection 5 min later (**Fig. S15**). The pretreatment of NG can inhibit the luminescent signal in NF-κB reporter mice even more effectively (**Fig. S15a-c**) than post-LPS NG treatment (**Fig. 6**), due to the presence of TD-NG for simultaneous LPS capture. At 4 h post injection, the NG pre-treatment showed a significant decrease of proinflammatory cytokine, including TNF-α and IL-6 (**Fig. S15d&e**). The results indicate that NG can neutralize both LPS and proinflammatory cytokine in the bloodstream for sepsis prevention.

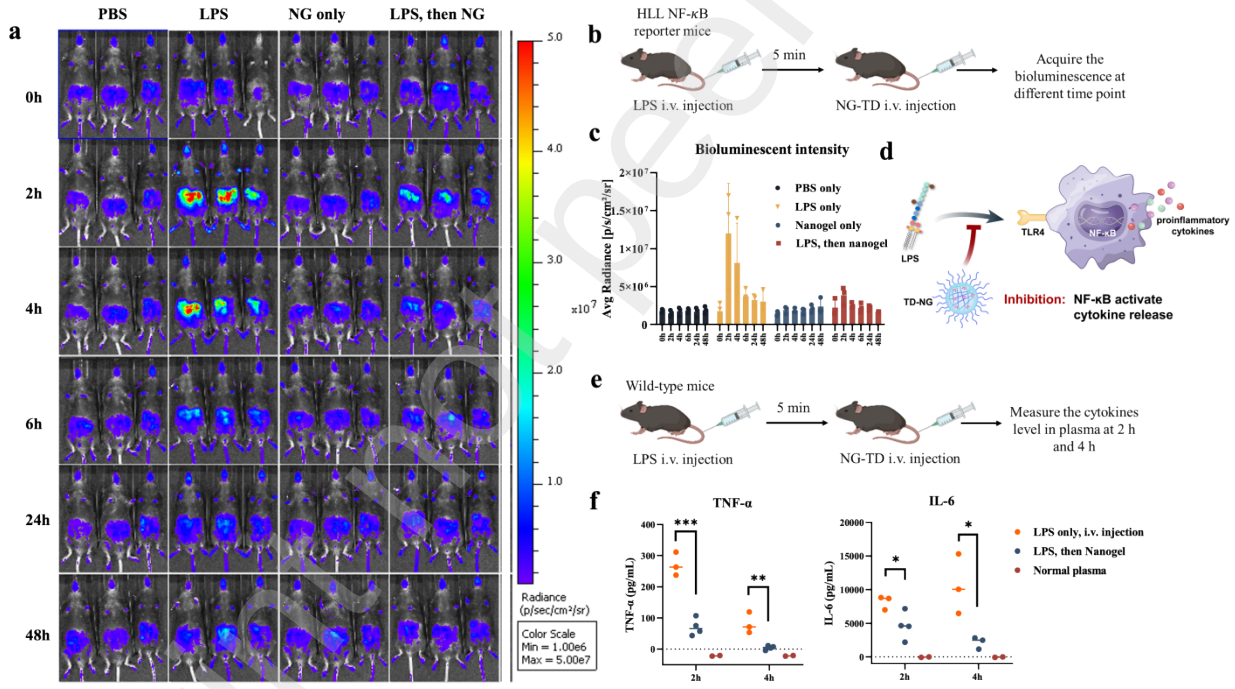

Figure 6. (a) Real-time in vivo bioluminescent imaging of the HLL NF-κB reporter mice recorded at different time points (b) after i.v. injections of NG (50 mg/kg) or PBS 5 min following i.v. injection of LPS (0.1 mg/kg). Bioluminescence was acquired by in vivo imaging system (Ami-HTX) 10 min after i.p. injection of luciferin solution (150 mg/kg) at t=0, 2, 4, 6, 24, 48 h; (c) the quantitative bioluminescent analysis of the HLL mice recorded different time points

(n = 3, mean ± SD); (d) schematic illustration of TD-NG inhibited the NF-κB activation and inflammatory responses to LPS stimulation; (e) experimental procedures for the LPS induced infection model with wild type mice. NG (50 mg/kg) or PBS were i.v. injected into mice 5 min after i.v. injection of LPS (0.1 mg/kg). Blood was collected from tail vain at 2 h and 4 h after LPS injection for ELISA test; (f) key cytokines TNF-α and IL-6 in plasma of PBS and NG treated groups compare with normal mice (n=3-4, mean ± SD).

CLP-induced polymicrobial sepsis treated by TD-NG

Cecal ligation and puncture (CLP), a murine model of bacterial peritonitis, recapitulates key features of secondary bacterial peritonitis in humans, including polymicrobial infection, persistently elevated circulating DAMPs, hyperdynamic circulatory system, and the development of acute lung injury is regarded as the clinically equivalent animal model of sepsis.[29,30] The nanogel was i.v. injected into mice 1 h after the CLP surgery, and followed by four daily doses from day 2 to day 5 (**Fig. 7a**) at 50 mg/kg. As show in **Figure 7b**, CLP surgery induced the severe sepsis and most of the mice dead within 5 days with survival around 11% on day 14. The TD-NG treatment significantly improved survival of mice from CLP-induced polymicrobial and the survival was around 80% by day 14. 24 h after the CLP surgery, the blood from each group were collected from the tail vain to evaluate the cytokine level by ELISA (**Fig. 7c&d**). Compared with the normal and sham mice, the CLP surgery could significantly increase both TNF-α and IL-6 in blood 24 h post treatments, and the mortality events were concentrated in 24 h post CLP caused by hyperinflammatory reactions. The NG treatment can effectively attenuate the level of proinflammatory cytokines, e.g., TNF-α and IL-6 (**Fig. 7c&d**) and prolong the survival, indicating that the reduced hyperinflammation at the acute phase of sepsis is essential for the survival (**Fig. 7b**). The body temperature and body weight of the survived mice were recorded over time (**Fig. 7e&f**). The nanogel treatment can reduce the hypothermia of the CLP mice. The survived mice showed body weight loss around 10-20% at first few days, then gradually recovered from day 5 in NG treated group.

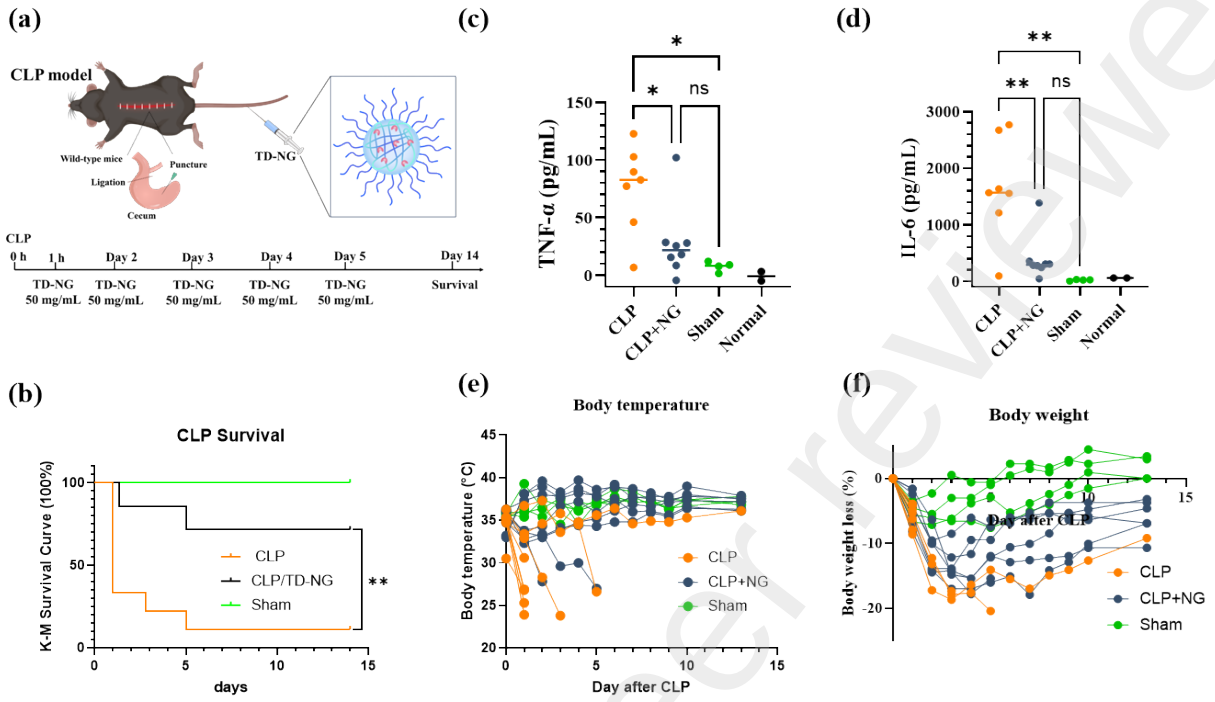

Figure 7. (a) Schematic illustration of sepsis mouse model induced by CLP surgery, and the treatment with TD-NG (10% $PEG^{5k}C17_4Arg_4$). The mice were administrated with TD-NG (50 mg/kg) at 1h, day 2, day 3, day 4 and day 5 post CLP by i.v. injection; (b) The survival of the CLP mice (n=8-9) with or without treatment with TD-NG monitored in 14 days; the cytokines of (c) TNF-α and (d) IL-6 in plasma collected through tail vain 24 h post CLP; (e) body temperature and (f) body weight of the survived CLP mice in 14 days.

Three mice from each group were sacrificed at 24 h post CLP for histology study to examine organ damages. H&E staining revealed obvious pathological changes and tissue damages in multiple organs in severe septic mice (**Fig. 8a**). Significant intra-alveolar hemorrhage with many red blood cells (RBCs, black circled) and alveolar thickening (black arrow) were observed in CLP mice, which indicated the acute lung injury (ALI). Concurrently, proximal tubular edema and vacuolization (black arrow), tubular epithelial cell simplification (blue circle) were observed in the CLP mice, indicating tubular injury in the kidney. In addition, intracellular edema and contraction bands (blue arrow) in cardiomyocytes, significant steatosis and vacuolization (blue

arrow) and foci inflammatory cells infiltration (black arrow) in liver, submucosa necrosis (blue circle) in intestine were observed in CLP mice, indicating multiple organ damage and possible mortality. It was noticed that the NG treatment can improve histopathology in all organs, which showed similar morphology as sham group. Quantification of typical biomarkers associated with kidney (creatinine and BUN) and liver (AST) functions showed no abnormally increased levels for the CLP TD-NG-treated animals in comparison to those in normal mice (**Fig. 8b-d**); notably increased biomarkers reveal liver and kidney injuries in CLP mice without treatments.

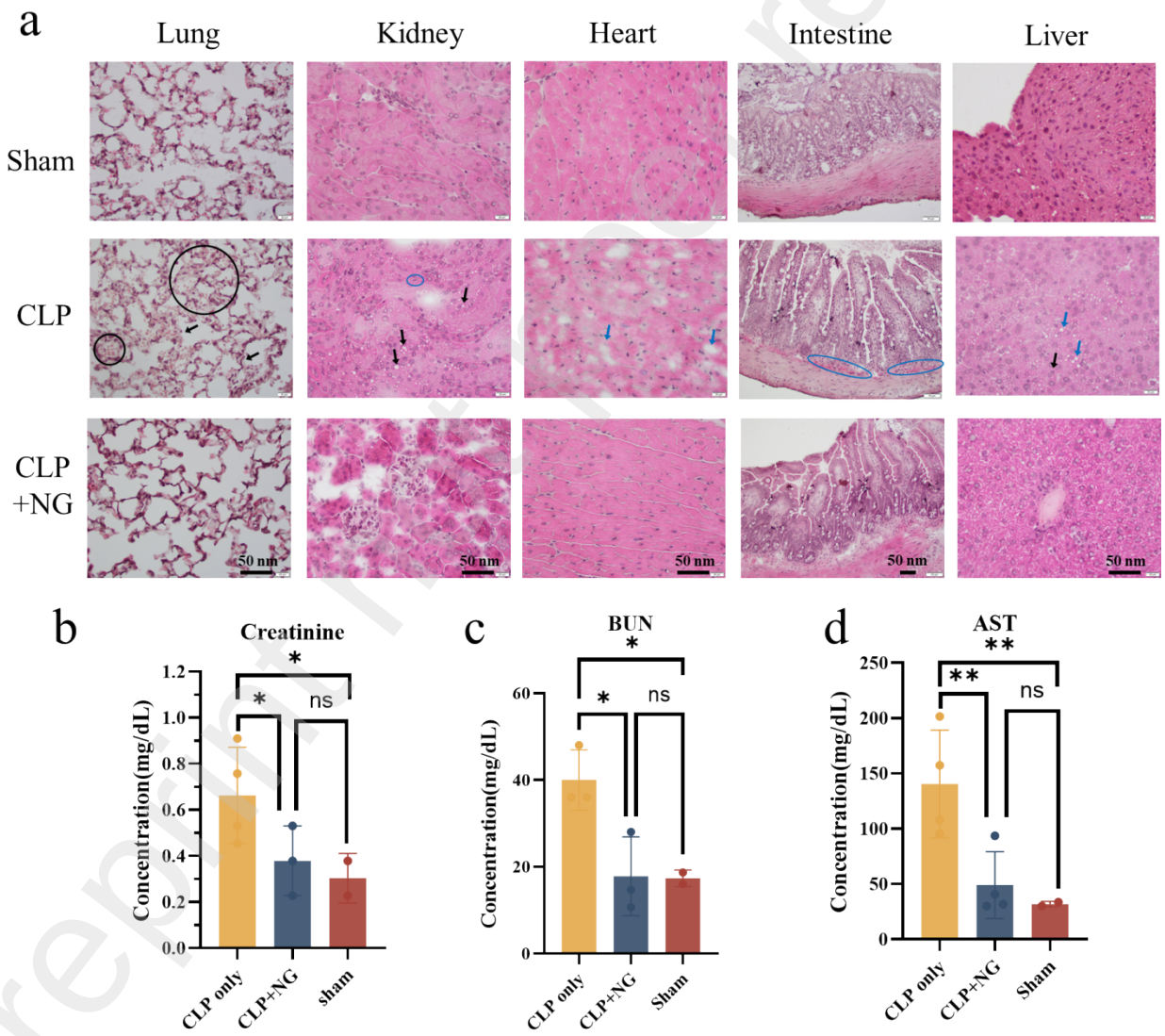

Figure 8. (a) Tissue histology stained with hematoxylin and eosin for major organs of septic mice in different treatment groups. Histopathological findings: Lung: alveolar hemorrhage (black circle) and thickening (black arrow); Kidney: proximal tubular edema and vacuolization (black arrow), tubular epithelial cell simplification (blue circle); Heart: intracellular edema and contraction bands (blue arrow); Intestine: submucosa necrosis (blue circle); Liver: predominantly macrovascular steatosis (blue arrow) and foci inflammatory cells infiltration (black arrow); Serum levels of the kidney function indicators blood (b) creatinine and (c) urea nitrogen (BUN) and (d) aspartate transaminase (AST) in mice of different treatment groups.

Discussion

Sepsis is systemic dysregulation of hyperimmune response to infection and tissue damages. The control of the source of pathogenesis within the local tissue is critical for sepsis prevention. Sepsis progress when the pathogen or immune-stimulating DAMPs and DAMPs spread into circulation, causing the systemic immune response, remote organ damage, multiple organ failures and death. Glucocorticoid therapy has long controversy history in the clinic for sepsis treatment, mainly due to the immune suppression and risk of secondary infection. The spontaneous attenuation of the cytokines and DAMPs/PAMPs in the circulation via hemoperfusion or blood filtration have been extensively explored in the clinic for sepsis treatment. However, no significant survival benefit in clinical trials was observed for such approaches, due to the heterogenous patient population, as well as the low efficiency of the extracorporeal blood clearance. In addition, the spontaneous inflammation control in the disease sites and other vital organs is critical to prevent the systemic hyperinflammation and reserve the immune system for effective infection control. Instead of relay on blood-tissue equilibrium, our TD nanogel could spontaneous scavenge circulating and potential tissue residential septic molecules after intravenous injection, given the leaky blood vessels and increased permeability in the infected and inflamed tissue/organs.

The general concern for the injectable nanogel is the biodegradability and elimination. There may be a concern about the slow cytokines/DAMPs/PAMPs release during TD-NG degradation for possible prolonged or chronic inflammation. Firstly, we believe that the scavenging or

reducing the overflowing levels of septic molecules (LPS or cytokines) is critical to prevent the hyperinflammation and immune dysregulation for better sepsis outcome. Secondly, the degradation of TD-NG likely occurs only in the endosome or lysosome, where cytokines and LPS will be degraded spontaneously, avoiding further immune stimulation. Therefore, we chose ethylene glycol based thermal sensitive monomer for nanogel synthesis with the redox sensitive disulfide bond containing crosslinker. As shown in **Fig. 1**, TD-NG is biodegradable with the challenge of reducing reagents, including glutathione (**Fig. S7**). TD-NG with the optimized crosslinking degree provides a critical size-exclusive effect against large and abundant serum proteins but allows smaller-sized cytokines and LPS to penetrate and capture (**Fig. 2c&d**). As demonstrated, TD-NG could selectively attenuate both LPS and proinflammatory cytokines via the combination of charge and hydrophobic interactions in both cell culture medium and animal and patient plasma (**Fig. 2&3**). The PEG polymer chains in TD display on the surface of nanogel to shelter the charges and hydrophobic domains in TD nanotrap, thus reducing the nonspecific protein binding and phagocytosis of NG (**Fig. 4**). Accordingly, TD-NG exhibits a substantial half-time in blood circulation *in vivo* ($t_{1/2}$ ~7 h). Interestingly, TD-NG was mainly excreted into feces (**Fig. 5**), although the particle size of NG (~300 nm) is significantly larger than the sinusoidal fenestration in liver (150-200 nm).[31,32] It is known that the exogenous nanoparticle, even with PEGylation, are ultimately taken up by phagocytes, e.g., Kupffer cell in liver. It is more likely that TD-NG is up taken first by Kupffer cells and partially digested via disulfide bond cleavage before excretion into the circulation, then extravasate the endothelium of sinusoidal fenestration. Hepatocyte further uptakes the TD-NG fragments for further metabolism and secretion into the bile duct for elimination.

We have demonstrated the effective attenuation of LPS and cytokines in cell culture and body fluids after *in vitro* TD-NG coincubation. It is more challenging to recapitulate the same efficacy *in vivo*, given the complex *in vivo* plasma proteins and cell/tissue components for LPS and cytokine binding. We first applied a prophylactic sepsis model by injecting TD-NG prior to LPS into mice. HLL mice have a luciferase transgene as the reporter for NF-κB activation, thus were used in LPS stimulation. Both bioluminescent imaging and cytokine analysis revealed that TD-NG was very effective in preventing LPS-induced inflammation *in vivo* (**Fig. 6&S15**), demonstrating efficient *in vivo* LPS attenuation from blood circulation. LPS is known as a very potent PAMP, which may readily bind to TLR4/MD2 receptor complex on immune cells and

endothelium cells[33] after i.v. injection to trigger cytokine productions. The early proinflammatory cytokines induced by LPS, e.g., TNF-α and IL-1β, further propagate inflammatory reactions. Thus, we further tested the efficacy of TD-NG in a sepsis mouse model 5 min after LPS stimulation. Although NF-κB activation can be still noticed in the post treatment group, which was significantly lower than the LPS group. Similarly, cytokine productions were also significantly reduced by TD-NG treatment in the wild type mice with the same experimental design, which may be attributed to both LPS and cytokines attenuation.

CLP mouse model comprises the polymicrobial infection and ischemic injury, replicating the feature of severe clinical sepsis. Although antibiotics are essential in the clinic to manage sepsis, we purposely omit the antibiotics in the treatment to check the survival benefit solely by TD-NG immune modulation. It is well understood that hyperinflammation propel the sepsis progression and multiple organ failures and death. At the same time, the dysregulated immune system can be exhausted to clear up infections. Thus, the reduced hyperinflammation in sepsis could both prevent organ failure and restore strong immune defense for infection control. The severeness of CLP mouse model can be generally controlled by the dose of tissue damage and the amount of fecal contamination. We adopted a CLP model with mortality rate about 60% after 48 hours and 10-20% survival eventually. We purposely start TD-NG treatment 1 h later after CLP procedure to allow the initiation of normal protective immune response, which is critical for survival benefit of immune modulation according to our previous study.[16] As expected, TD-NG treatment significantly increase the survival rate, which is supported by attenuated cytokine production, improved body temperature control, and reduced tissue damages in both histology and blood chemistry analysis (**Fig. 7&8**).

Conclusion

In this project, we developed a nanogel with telodendrimer (TD-NG) for selective adsorption of septic molecules as effective immune modulation. The polymerizable PEGylated TD enables the one-pot preparation of biodegradable TD-NG with clean and biocompatible surface chemistry for intravenous injection in sepsis treatment. The introduction of dendritic binding clusters combining both positive charges and hydrophobic moieties in the core of nanogel enables the

effective adsorption of LPS and pro-inflammatory cytokines both *in vitro* and *in vivo* in mouse models. We have demonstrated that the TD-NG treatment can significantly improve the survival in CLP mice. Such TD-NG can be further engineered in future to encapsulate antibiotics for spontaneous control of both infection and hyperinflammation to further improve sepsis treatment. In addition, such TD-NG has great potential in the treatment of other diseases and medical conditions with high risk of cytokine storm, for example, trauma, burn, severe cardiac surgery, pancreatitis and CAR-T therapy.

Contributions

J.L. and X.J., designed the project and experiments. X.J., C.S., D.Y., L.S., X.Y., and M.R. conducted the experiments and collected the data. D.G., N.U. and R.C. helped with reagents and material. L.S., N.R. and R.C. provided input for data interpretation. X.J. and J. L wrote the paper.

Competing interests

The authors declare no competing interests.

Acknowledgement

We greatly acknowledge the financial support from NIH/NIGMS R35GM153495-01 (Luo), DOD/TTDA PR221368 (Luo), NY FIRST fund (Luo), Maureen T. O'Hara TEAL THERE's A CURE, and Christine Schoeck Blakely Ovarian Cancer Research Foundation (Luo). Biorender was used to create some schematic illustrations.

Data Availability Statement

The data that support the findings of this study are available in the supplementary material of this article.

Reference

1. Angus, D.C. & Van der Poll, T. Severe sepsis and septic shock. *N Engl J Med* **369**, 840-851 (2013).
2. Papafilippou, L., Claxton, A., Dark, P., Kostarelos, K. & Hadjidemetriou, M. Nanotools for sepsis diagnosis and treatment. *Advanced Healthcare Materials* **10**, 2001378 (2021).
3. Hung, Y.-L*., et al.* Corylin protects LPS-induced sepsis and attenuates LPS-induced inflammatory response. *Scientific reports* **7**, 1-11 (2017).
4. Brandenburg, K*., et al.* An update on endotoxin neutralization strategies in Gram-negative bacterial infections. *Expert Review of Anti-infective Therapy* **19**, 495-517 (2021).
5. Buttenschoen, K., Radermacher, P. & Bracht, H. Endotoxin elimination in sepsis: physiology and therapeutic application. *Langenbeck's archives of surgery* **395**, 597-605 (2010).
6. Pfalzgraff, A. & Weindl, G. Intracellular lipopolysaccharide sensing as a potential therapeutic target for sepsis. *Trends in pharmacological sciences* **40**, 187-197 (2019).
7. Munford, R. Detoxifying endotoxin: Time, place and person. *Journal of Endotoxin Research* **10**, 16 (2004).
8. van der Poll, T., Shankar-Hari, M. & Wiersinga, W.J. The immunology of sepsis. *Immunity* **54**, 2450-2464 (2021).
9. Yoo, W*., et al.* Nanodiamond as a Cytokine Sponge in Infectious Diseases. *Frontiers in bioengineering and biotechnology*, 504 (2022).
10. Bertani, B. & Ruiz, N. Function and biogenesis of lipopolysaccharides. *EcoSal Plus* **8**(2018).
11. Messina, J.M*., et al.* Unveiling cytokine charge disparity as a potential mechanism for immune regulation. *Cytokine Growth Factor Rev* **77**, 1-14 (2024).
12. Zampieri, F.G*., et al.* Relationship between acid–base status and inflammation in the critically ill. *Critical Care* **18**, 1-8 (2014).
13. Wang, L*., et al.* Zwitterionic Janus Dendrimer with distinct functional disparity for enhanced protein delivery. *Biomaterials* **215**, 119233 (2019).
14. Wang, X*., et al.* Structure-Based Nanocarrier Design for Protein Delivery. *ACS Macro Letters*, 267-271 (2017).
15. Wang, X*., et al.* Affinity-controlled protein encapsulation into sub-30 nm telodendrimer nanocarriers by multivalent and synergistic interactions. *Biomaterials* **101**, 258-271 (2016).
16. Shi, C*., et al.* A nanotrap improves survival in severe sepsis by attenuating hyperinflammation. *Nature Communications* **11**, 3384 (2020).
17. Ji, X*., et al.* Functionalized Core–Shell Nanogel Scavenger for Immune Modulation Therapy in Sepsis. *Advanced Therapeutics*, 2200127 (2022).
18. Tamburro, D*., et al.* Multifunctional core–shell nanoparticles: Discovery of previously invisible biomarkers. *Journal of the American Chemical Society* **133**, 19178-19188 (2011).
19. Blackburn, W.H. & Lyon, L.A. Size-controlled synthesis of monodisperse core/shell nanogels. *Colloid and polymer science* **286**, 563-569 (2008).
20. Longo, C*., et al.* Core-shell hydrogel particles harvest, concentrate and preserve labile low abundance biomarkers. *PloS one* **4**, e4763 (2009).
21. Guo, D*., et al.* Rationally designed micellar nanocarriers for the delivery of hydrophilic methotrexate in Psoriasis treatment. *ACS applied bio materials* **3**, 4832-4846 (2020).
22. Wang, L., Ji, X., Guo, D., Shi, C. & Luo, J. Facial Solid-Phase Synthesis of Well-Defined Zwitterionic Amphiphiles for Enhanced Anticancer Drug Delivery. *Molecular Pharmaceutics* **18**, 2349-2359 (2021).
23. Caroff, M. & Novikov, A. LPS structure, function, and heterogeneity. *Endotoxin detection and control in pharma, limulus, and mammalian systems*, 53-93 (2019).
24. Guo, D., Ji, X. & Luo, J. Rational nanocarrier design towards clinical translation of cancer nanotherapy. *Biomedical Materials* **16**, 032005 (2021).

25. Li, X.*, et al.* Redox/temperature responsive nonionic nanogel and photonic crystal hydrogel: comparison between N, N'-Bis (acryloyl) cystamine and N, N'-methylenebisacrylamide. *Polymer* **137**, 112-121 (2018).
26. Opal, S.M.*, et al.* Relationship between Plasma Levels of Lipopolysaccharide (LPS) and LPS-Binding Protein in Patients with Severe Sepsis and Septic Shock. *The Journal of Infectious Diseases* **180**, 1584-1589 (1999).
27. Nordgreen, J.*, et al.* The effect of lipopolysaccharide (LPS) on inflammatory markers in blood and brain and on behavior in individually-housed pigs. *Physiology & behavior* **195**, 98-111 (2018).
28. Ren, Y.*, et al.* Apoptotic cells protect mice against lipopolysaccharide-induced shock. *The Journal of Immunology* **180**, 4978-4985 (2008).
29. Das, P.*, et al.* Novel chitohexaose analog protects young and aged mice from CLP induced polymicrobial sepsis. *Scientific reports* **9**, 1-12 (2019).
30. Remick, D.G., Newcomb, D.E., Bolgos, G.L. & Call, D.R. Comparison of the mortality and inflammatory response of two models of sepsis: lipopolysaccharide vs. cecal ligation and puncture. *Shock* **13**, 110-116 (2000).
31. Cogger, V.C., O'Reilly, J.N., Warren, A. & Le Couteur, D.G. A standardized method for the analysis of liver sinusoidal endothelial cells and their fenestrations by scanning electron microscopy. *J Vis Exp*, e52698 (2015).
32. Zhang, Y.-N., Poon, W., Tavares, A.J., McGilvray, I.D. & Chan, W.C.W. Nanoparticle–liver interactions: Cellular uptake and hepatobiliary elimination. *Journal of Controlled Release* **240**, 332-348 (2016).
33. Stierschneider, A. & Wiesner, C. Shedding light on the molecular and regulatory mechanisms of TLR4 signaling in endothelial cells under physiological and inflamed conditions. *Front Immunol* **14**, 1264889 (2023).